

Improvement of Electrical Conductivity with Phase-Separation in Polyolefin/Multiwall Carbon Nanotube/Polyethylene Oxide Composites

Kensuke Miyazaki, Noriyasu Okazaki, Hisayuki Nakatani

Department of Biotechnology and Environmental Chemistry, Kitami Institute of Technology 165 Koen-cho, Kitami, Hokkaido 090-8507, Japan

Correspondence to: H. Nakatani (E-mail: nakatani@chem.kitami-it.ac.jp)

ABSTRACT: Electrical conductivity developments of polypropylene (PP)/multiwall carbon nanotube (MWNT) and polybutene (PB)/MWNT composites were carried out with polyethylene oxide (PEO) phase-separation behavior for the polymeric materials. The low conductivity ($8.47 \times 10^{-8} \text{ S cm}^{-1}$) of PP(98%)/MWNT (2%) was drastically increased up to $1.56 \times 10^{-3} \text{ S cm}^{-1}$ by only 2% PEO(96%)/MWNT(4%) loading. The drastic improvement originated from the formation of an electrical connector structure with the PEO/MWNT domain. The PB(93%)/MWNT(7%) conductivity was also improved by the PEO(92%)/MWNT(8%) loading although the conductivity improvement effect was lower than that of the PP/MWNT. The Raman spectra showed that the MWNT dispersity in the PB was poorer than that in the PP, resulting in the formation of a PEO/MWNT connector structure only at higher loading. In addition, a PEO/carbon black composite was able to produce the connector structure for the PP/MWNT as well as the PEO/MWNT. These results indicated that the highly conductive composites could be produced with smaller MWNT amounts. © 2012 Wiley Periodicals, Inc. *J. Appl. Polym. Sci.* 128: 3751–3757, 2013

KEYWORDS: composites; nanotubes; graphene and fullerenes; polyolefins; phase behavior

Received 7 June 2012; accepted 14 September 2012; published online 10 October 2012

DOI: 10.1002/app.38591

INTRODUCTION

Carbon nanotube (CNT) is one of attractive fillers for polymer composite from the viewpoints of good electrical,¹ mechanical,^{2,3} and thermal⁴ properties. Because CNT has a high aspect ratio, even the small loading amount allows these properties to be strongly improved.^{5–7} CNT is a long length structure, resulting that the entanglement occurs. The entanglement brings about a three-dimensional network structure (percolation) of CNT. The formation of the CNT percolation in the polymer composite brings about considerable improvement in the electrical conductivity even with a small amount of the loading.^{8–11} The electrical conductivity has a sizeable step of several orders of magnitude above a CNT weight fraction.^{8,10} This electrical behavior is due to the CNT percolation formation, and the CNT weight fraction is called as the “percolation threshold.”^{8–11} The percolation threshold strongly depends on dispersity and/or alignment of the CNT in the polymer matrix.⁹ In addition, the threshold depends on kinds of the polymer matrix. For instance, in the cases of polyethylene (PE) and polyepoxy matrices, the percolation thresholds were reported to be about 2 wt %¹⁰ and about 0.0025 wt %, respectively. The polymer coat intercepts the CNT–CNT contact, resulting that

higher concentration of the CNT is required to reach the threshold.⁹ Therefore, the threshold certainly depends on the surface coverage by the polymer matrix. If there is some interaction between the CNT and the polymer, the surface coverage is more likely to increase, and the threshold is raised. The contact of uncoated CNTs is required to lower the threshold.

An application of phase separation between polymers has a potential to prevent CNT surface from polymer coating. The CNT in the interface would hardly be coated due to repulsion between the polymers. Therefore, the phase separation gives the contact of uncoated CNTs at the interface. If the phase-separated polymer/CNT domain has electrical conductivity, it becomes an electrical connector among the CNTs in the polymer matrix. The size and/or dispersity control of such connector certainly leads to lower the threshold.

In this work, electrical conductivity developments of PP/MWNT and PB/MWNT have been carried out with PEO phase-separation behavior for the polymeric materials. The PEO/MWNT loading effects have been assessed in the conductivity, and the changes of these percolation threshold values have been studied. The formation of the PEO/MWNT connector structure and the MWNT aggregation behavior has been evaluated by

electron microscope and Raman spectra measurements. In addition, the loading effects of two kinds of carbon black have been studied in terms of the formation of the connector structure as well as MWNT.

EXPERIMENTAL

Raw Materials

PP was supplied by Japan Polypropylene. The number-average molecular weight (M_n) and the polydispersity (M_w/M_n) of the PP were 4.6×10^4 and 5.7, respectively. PB was supplied by Japan Polychem. The number-average molecular weight (M_n) and the polydispersity (M_w/M_n) were 1.0×10^5 and 5.2, respectively. PEO was purchased from Wako Pure Chemical Industries. The average molecular weight was 5.0×10^5 .

MWNT was synthesized through the dissociation of methane at 750°C with a Fe_2O_3 catalyst. The diameter was from about 20–80 nm, and the length was from about 0.1–3 μm (these values were obtained from the tenth MWNT samples).¹² Two kinds of acetylene black (Ketjenblack carbon EC300J and Denka black) were supplied by Lion and Denki Kagaku Kougyou and were denoted as KB and DB, respectively. The diameters of KB and DB were 39.5 and 35 nm, respectively.

Sample Preparations

All composite samples were carried out with an Imoto Seisakusyo IMC-1884 melting mixer. The polymer/carbon material composites were mixed at 180°C for the PP composite and 150°C for PB one at 100 rpm for 5 min.

These film preparation was carried out with a compress-molding. All composites were molded for 8 min at 180 or 150°C under 10 MPa and then were quickly quenched up to room temperature (ca. 20°C). All measurements were carried out with the films.

Electrical Conductivity Measurement

The electrical conductivity of the film samples with 100 μm thickness was determined at room temperature by a conventional four-point-probe technique with a resistivity meter (Lorsta-GP MCP-T610, Mitsubishi Chemical).

Scanning Electron Microscope (SEM) Observation

SEM observation was carried out with a JEOL JSM-5800 and a JSM-6701 F (Field emission-SEM (FE-SEM)) at 5–8 kV. In the case of the SEM observation at the cross section of the composite sample, the sample was prepared by the fracture of about 800- μm thick compression molded film in liquid nitrogen, whereas, in the case of the SEM observation at the surface of the composite sample, the compression molded film surface was used without treatment. These samples were sputter-coated with gold and were measured.

Raman Spectrometer Measurement

Raman spectra were obtained at room temperature with a JASCO NR-1800 with 532 nm excitation wavelength (semiconductor laser, laser power 100 mW).

RESULTS AND DISCUSSION

Figure 1 showed the electrical conductivity of the PP/MWNT, PB/MWNT and PEO/MWNT as a function of the MWNT

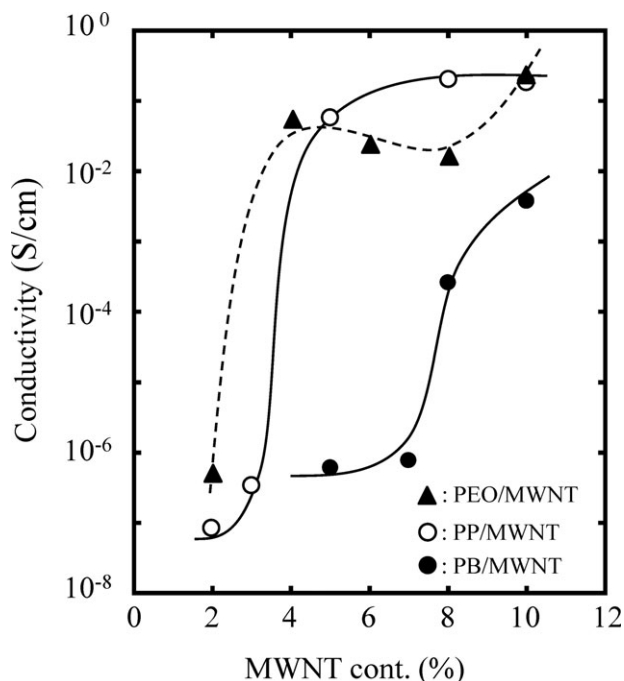


Figure 1. Electrical conductivity of PP/MWNT, PB/MWNT and PEO/MWNT composites as a function of MWNT loading: % = wt %.

loading. The PP/MWNT conductivity shows a drastic increase between the 3 and 5% of the MWNT content, suggesting that the MWNT percolation threshold is about 4%. The percolation thresholds of the PB/MWNT and PEO/MWNT are about 7.5 and 2.5%, respectively. Although PB is a kind of polyolefin as well as PP, there is a large difference in the percolation threshold between them. Figure 2 showed the SEM microphotographs cross section of the PB/MWNT and PP/MWNT. The PP/MWNT microphotograph shows the existences of many longer fibers. In addition, as shown in the high magnification of the SEM microphotograph, the uncoated MWNT fibers can be observed. In the case of the PB/MWNT microphotograph, many white dots and shorter fibers corresponding to some part of the MWNT are observed. As shown in Figure 3 the SEM microphotograph of the PP/MWNT surface distinctly shows the MWNT network structure, and it cannot be observed on the PB/MWNT surface. It reveals that the formation of the MWNT network structure is more difficult in the PB/MWNT. The PB chains adhere to the MWNT surface and interfere with the formation of the network structure. Therefore, more loading amount of the MWNT is required to form the network structure in the PB matrix. The percolation threshold of the PEO/MWNT is much lower than that of the PP/MWNT. The MWNT is well dispersible in PEO having polarity. The formation of MWNT network structure easily occurs, resulting that the percolation threshold lowers to the lower MWNT content.

MWNT network structure such as entanglement is required for conductivity appearance in MWNT composite, and its increasing the number certainly leads to lowering the threshold.¹³

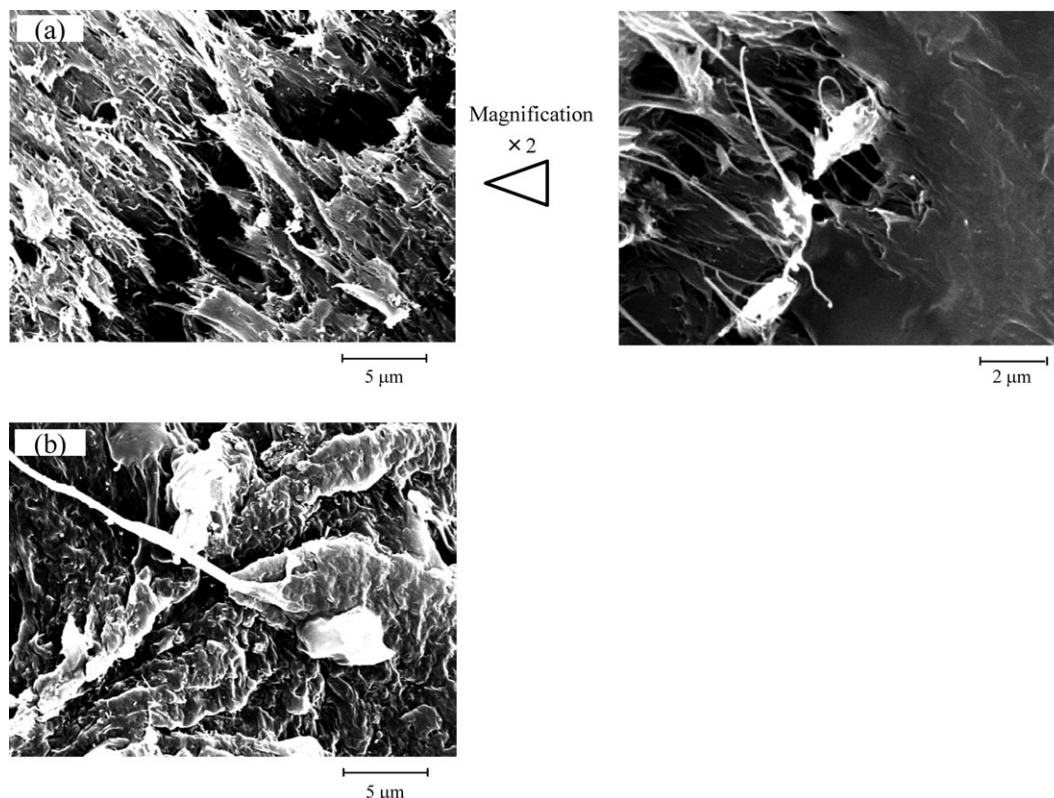


Figure 2. SEM microphotographs cross section of PB/MWNT and PP/MWNT of composites. (a): PP(90%)/MWNT(10%) (b): PB(90%)/MWNT(10%).

Shrivastava et al. reported that a use of polystyrene (PS) beads during bulk polymerization of MWNT/styrene lowered the percolation threshold in PS matrix without any surface modification of the MWCNT.¹³ The lowering was due to selective concentration of the MWNT in the matrix with MWNT exclusion effect of the PS beads. Such control method of the vacant space by phase-separation is useful for minimization of the MWNT percolation threshold. In this study, the threshold minimization of the PP and PB composites was performed by a similar method with phase-separation phenomenon. PP and PEO are incompatible blend.^{14–16} The polymer blend showed

microscopically phase-separated (sea-island) morphology, and its domain size depended on the PEO content.¹⁶ In addition, the PB/PEO blend is incompatible as well as PP/PEO one. It is noted here that our method for the threshold minimization uses not MWNT exclusion effect but connector one. Figure 4 showed the expression mechanism of PP/MWNT (PB/MWNT) conductivity with PEO/MWNT domain. The phase-separated PEO/MWNT has conductivity and works as electrical connector among free MWNT in the PP matrix. The MWNT network structure is formed not by the MWNT entanglement but by the connector.

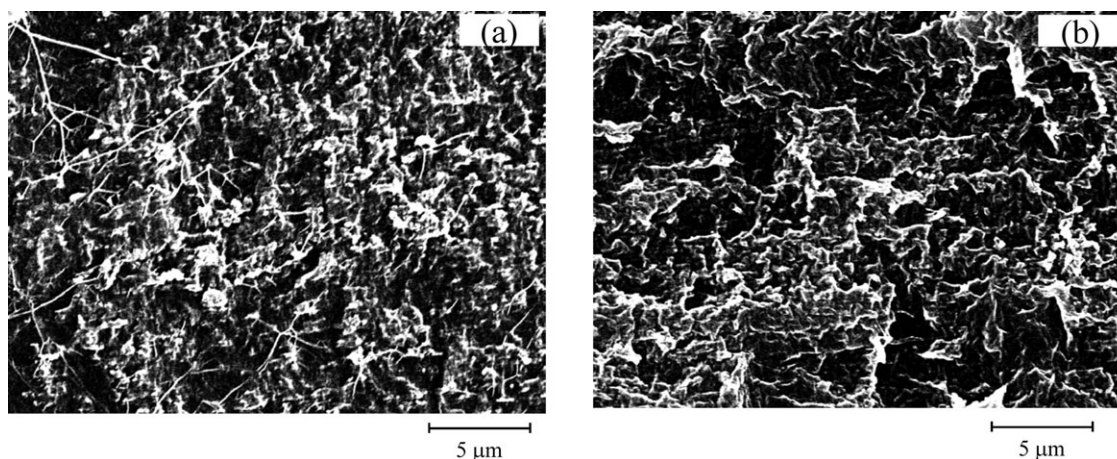


Figure 3. SEM microphotographs of surface of PP/MWNT and PB/MWNT of composites. (a): PP(90%)/MWNT(10%) (b): PB(90%)/MWNT(10%).

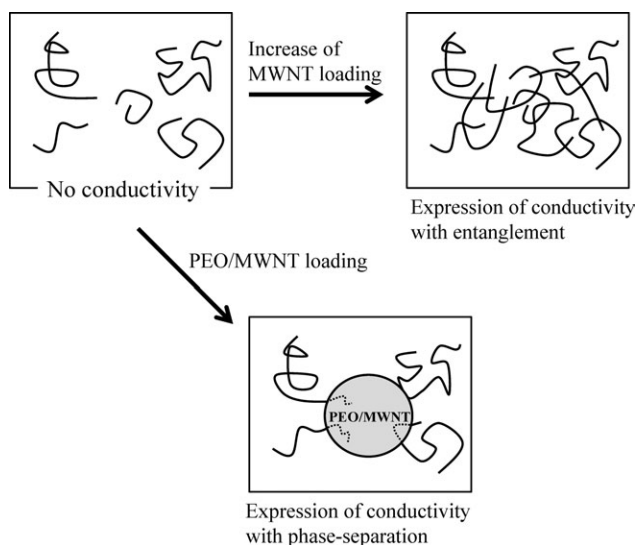


Figure 4. Expression mechanism of conductivity.

Figure 5 showed the electrical conductivity versus increment of total MWNT content (Δ total MWNT) in PP(98%)/MWNT(2%) + $n\%$ [PEO(96%)/MWNT(4%)] or + $n\%$ [PEO(92%)/MWNT(8%)] composites. The PEO/MWNT loading certainly brings about an improvement of the PP/MWNT conductivity. The MWNT percolation thresholds in the PP/MWNT was about 3% MWNT content, and the conductivity of the PP(98%)/MWNT(2%) was very low ($8.47 \times 10^{-8} \text{ S cm}^{-1}$). Only 2% loading (corresponding to Δ total MWNT = 0.04%) of the PEO(96%)/MWNT(4%) brings about the drastic increase of

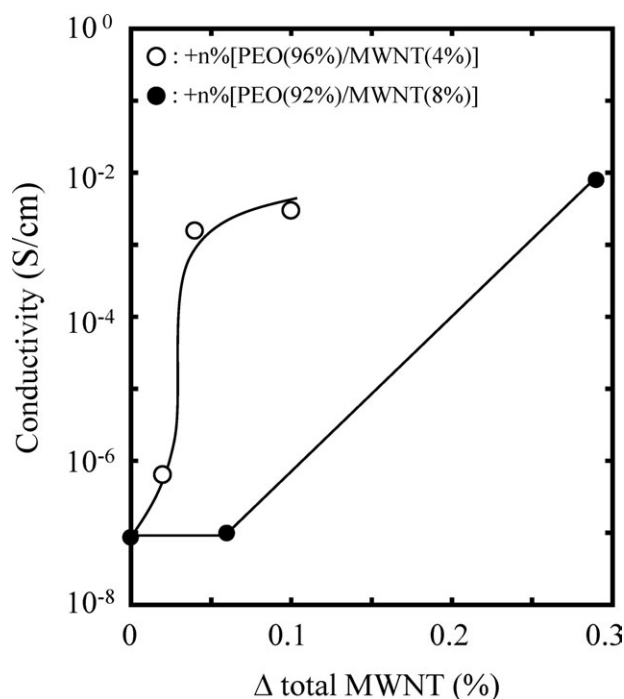


Figure 5. Electrical conductivity versus increment of total MWNT content (Δ total MWNT) in PP(98%)/MWNT(2%) + $n\%$ [PEO(96%)/MWNT(4%)] or + $n\%$ [PEO(92%)/MWNT(8%)] composites.

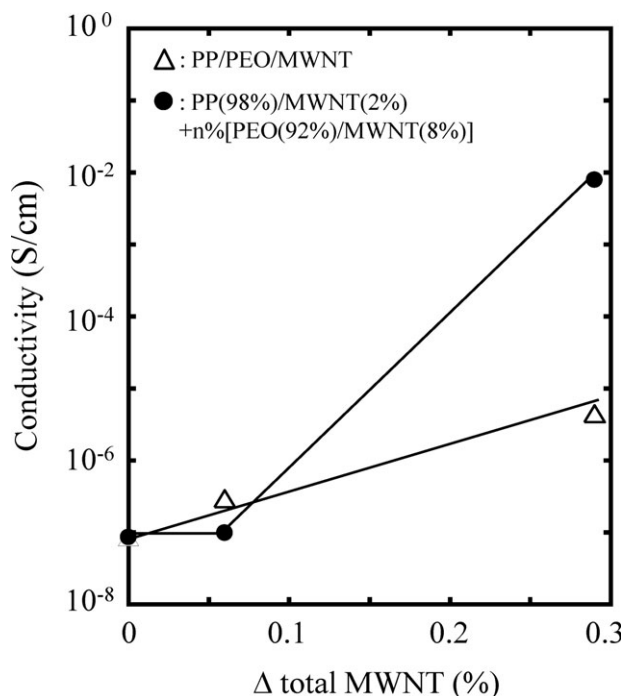


Figure 6. Electrical conductivity versus Δ total MWNT content in PP/PEO/MWNT and PP(98%)/MWNT(2%) + $n\%$ [PEO(92%)/MWNT(8%)] composites: Each of amount of PP, PEO, and MWNT is the same between both composites.

conductivity ($1.56 \times 10^{-3} \text{ S/cm}$). The improvement must be originated from the formation of MWNT network structure with the PEO(96%)/MWNT(4%) domain. The domain conductivity is $5.33 \times 10^{-2} \text{ S cm}^{-1}$, indicating that the domain is able to work as the connector among the MWNT in the PP matrix. The conductivity of PP(98%)/MWNT(2%) is drastically increased by the PEO(96%)/MWNT(4%) loading. The loading of the PEO(92%)/MWNT(8%) with $1.59 \times 10^{-2} \text{ S cm}^{-1}$ conductivity is effective for the conductivity increment of the PP(98%)/MWNT(2%) as well as that of the PEO(96%)/MWNT(4%), however, the small loading (corresponding to Δ total MWNT = 0.06%) does not show a clear effect for it. The PEO(92%)/MWNT(8%) domain is more rigid than the PEO(96%)/MWNT(4%) one because of its higher MWNT content. Therefore, it seems that it is a little hard to disperse the PEO(92%)/MWNT(8%) in the PP(98%)/MWNT(2%) matrix. The less dispersity requires the higher loading amount.

Figure 6 showed the electrical conductivity versus Δ total MWNT content in PP/PEO/MWNT and PP(98%)/MWNT(2%) + $n\%$ [PEO(92%)/MWNT(8%)] composites. These composites were obtained from simultaneous (PP/PEO/MWNT) and batch (PP(98%)/MWNT(2%) + $n\%$ [PEO(92%)/MWNT(8%)]) mixing methods with the same component content, respectively. As shown in Figure 6 the conductivity dependence on the Δ total MWNT is certainly different between both mixing methods. The increment rate of the conductivity in the PP/PEO/MWNT is considerably slower than that in the PP/MWNT + $n\%$ [PEO/MWNT]. It seems that diffusion rate of the MWNT component is not so high in the simultaneous mixing method.

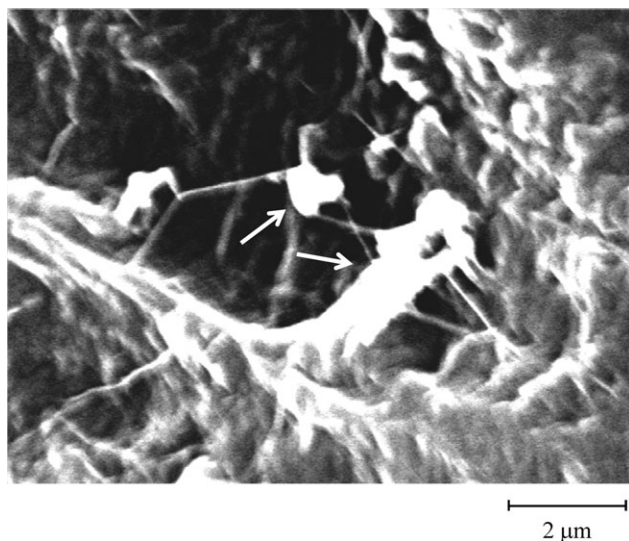


Figure 7. SEM microphotograph of PP(98%)/MWNT(2%) + 5%[PEO(92%)/MWNT(8%)] sample surface. Arrows indicate connector structure.

The formation rate of the PEO/MWNT domain connector must be slow. It is found that the batch mixing method is preferred for the formation of the connector. In fact, as shown in Figure 7 the existence of the connector structure can be observed in the PP/MWNT + 5%[PEO/MWNT].

Figure 8 showed the electrical conductivity versus Δ total MWNT content in PB(95%)/MWNT(5%) + n %[PEO(92%)/MWNT(8%)] and PB(93%)/MWNT(7%) + n %[PEO(92%)/MWNT(8%)] composites. The PEO/MWNT loading does not show the conduc-

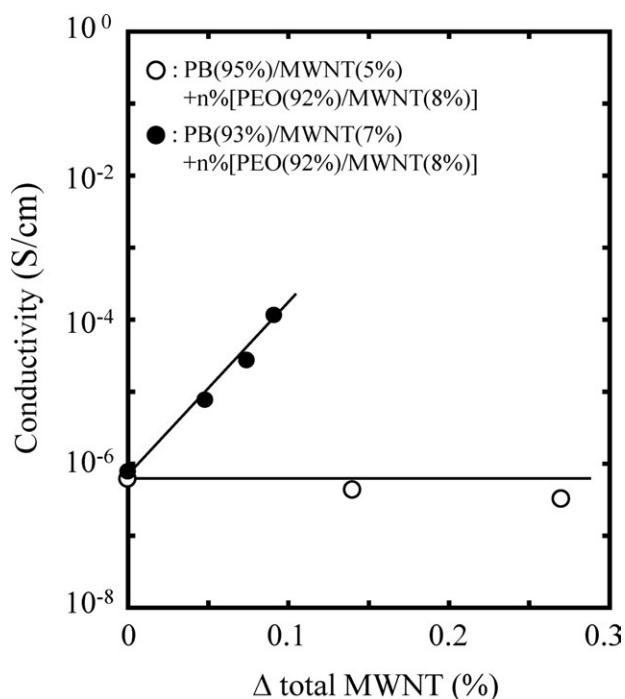


Figure 8. Electrical conductivity versus Δ total MWNT content in PB(95%)/MWNT(5%) + n %[PEO(92%)/MWNT(8%)] and PB(93%)/MWNT(7%) + n %[PEO(92%)/MWNT(8%)] composites.

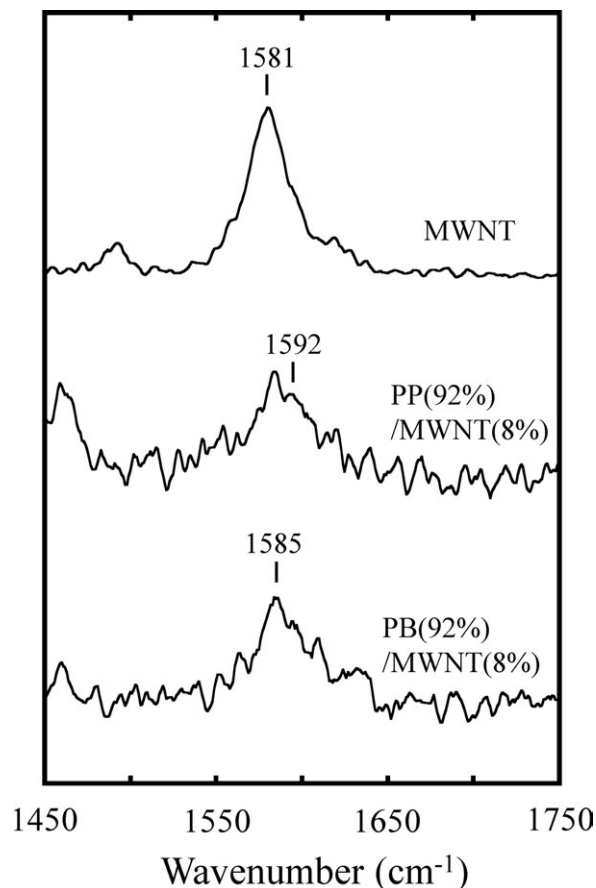


Figure 9. Raman spectra of MWNT bundles, PP/MWNT, PB/MWNT, and PB/MWNT in the range of 1450–1750 cm^{-1} (around G band peak).

tivity improvement of the PB(95%)/MWNT(5%) and brings about the slow increase of the PB(93%)/MWNT(7%) conductivity. These results suggest that it is hard to form the connector structure with the PEO/MWNT domain as compared with the PP/MWNT matrix. Figure 9 showed the Raman spectra of the MWNT bundles, PP(92%)/MWNT(8%) and PB(92%)/MWNT(8%) in the range of 1450–1750 cm^{-1} (around G band peak). The G band is originated from an in-plane vibration of C—C bond in MWNT¹⁰ and shifts to higher frequencies by the disentanglement of MWNT.^{9–11,17} The maxima in the G band in the MWNT bundles and PB(92%)/MWNT(8%) are located at 1581 and 1585 cm^{-1} , respectively. The maximum in the PP(92%)/MWNT(8%) is located at 1592 cm^{-1} , although another peak intensity around 1585 cm^{-1} can be observed. The MWNT dispersivity state in the PB matrix is lower than that in the PP one, and the MWNT is rather aggregated. The MWNT is bundled and is eccentrically located. The distance among the MWNTs in PB matrix must be considerably far, and the higher loading amount of the PEO/MWNT is required to form the connector among.

Figure 10 showed the relationship between the total MWNT content and conductivity of the MWNT composites. The PEO/MWNT loading certainly brings about the conductivity increments of the PP/MWNT and PB/MWNT composites and leads to the lowering of their MWNT percolation thresholds. For

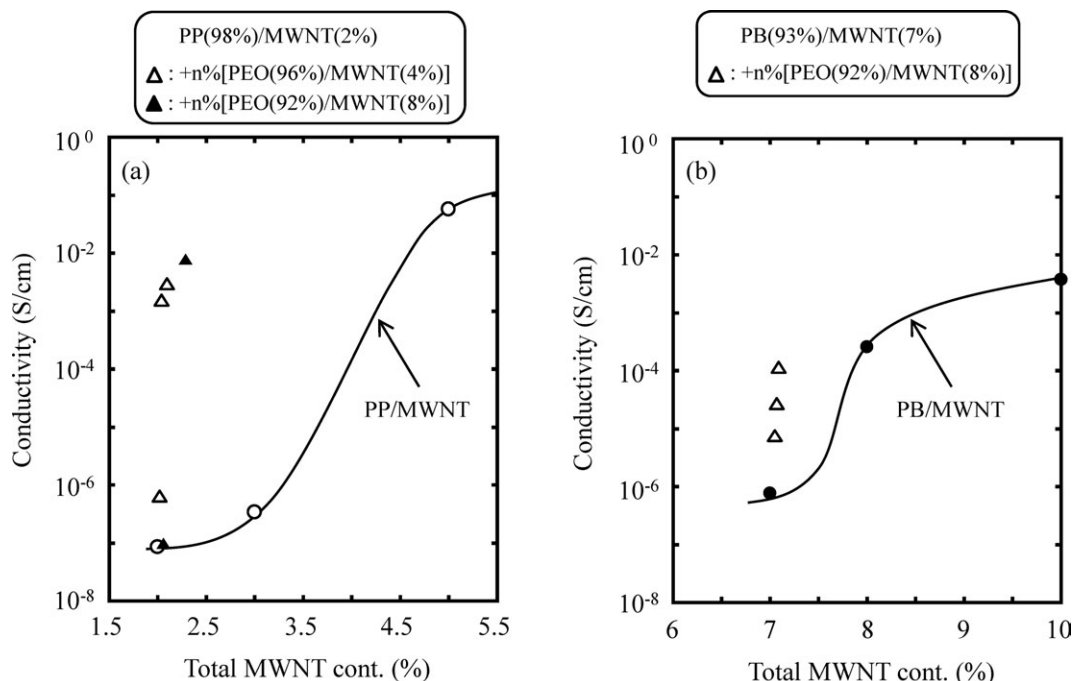


Figure 10. Electrical conductivity versus total MWNT content. (a): PP/MWNT, PP(98%)/MWNT(2%) + $n\%$ [PEO(96%)/MWNT(4%)] and PP(98%)/MWNT(2%) + $n\%$ [PEO(92%)/MWNT(8%)]. (b): PB/MWNT and PB(93%)/MWNT(7%) + $n\%$ [PEO(92%)/MWNT(8%)].

instance, the 2% PEO(96%)/MWNT(4%) and the 5% PEO(92%)/MWNT(8%) loadings increase the conductivity of PP(98%)/MWNT(2%) up to 1.56×10^{-3} S cm⁻¹ and 7.88×10^{-3} S cm⁻¹, respectively. The conductivity values are approximately equal to one-tenth of that of the PP(95%)/MWNT(5%), and the total MWNT contents are only 2.04 and 2.29% [ca. 41–46% total MWNT contents of PP(95%)/MWNT(5%)], respectively. The PB(93%)/MWNT(7%) shows a conductivity increment behavior as well as the PP(98%)/MWNT(2%), although the PEO/MWNT loading effect is relatively less. For instance, the 10% [PEO(92%)/MWNT(8%)] loading (7.09% total MWNT content) provides about 150 times higher value (1.15×10^{-4} S cm⁻¹) as compared with the PB(93%)/MWNT(7%). The PEO/MWNT loading develops the conductivity of the PP/MWNT and PB/MWNT, resulting that the usage of MWNT can be considerably reduced.

Carbon black is also a kind of conductive material and is more low-cost than MWNT. It seems that carbon black is able to

produce the connector structure as well as MWNT. The conductivity values of the PEO/MWNT, PEO/carbon black (KB) and PEO/carbon black (DB) were summarized in Table I. The conductivity (2.11×10^{-1} S cm⁻¹) of the PEO(90%)/KB(10%) is almost the

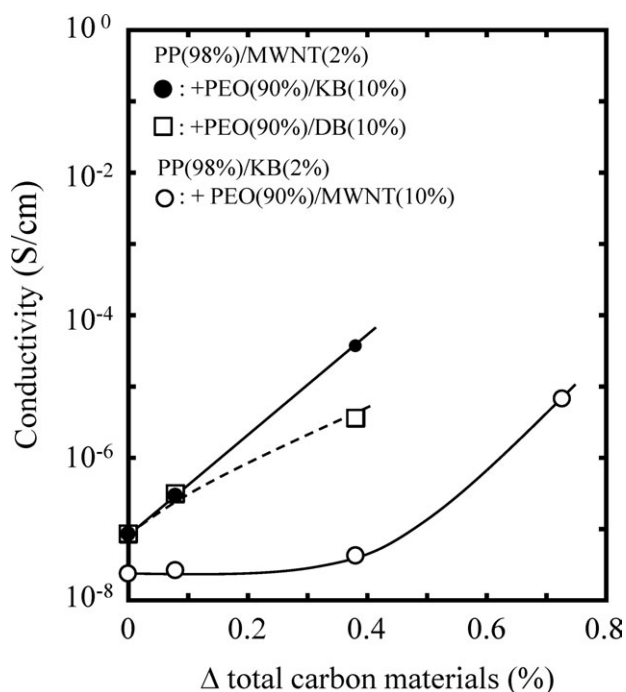


Figure 11. Electrical conductivity versus increment of total carbon materials content (Δ total carbon materials) in PP(98%)/MWNT(2%) + $n\%$ [PEO(90%)/KB(10%)] or + $n\%$ [PEO(90%)/DB(10%)] and in PP(98%)/KB(2%) + $n\%$ [PEO(90%)/MWNT(10%)] composites.

Table I. Conductivity of Some Carbon Material Composites

Composites	Content of carbon material (%)	Conductivity (S/cm)
PEO(98%)/MWNT(2%)	2	4.92×10^{-7}
PEO(90%)/MWNT(10%)	10	2.00×10^{-1}
PP(98%)/MWNT(2%)	2	8.47×10^{-8}
PEO(10%)/KB(10%)	10	2.11×10^{-1}
PEO(10%)/DB(10%)	10	2.45×10^{-6}
PP(98%)/KB(2%)	2	2.36×10^{-8}

same as that ($2.00 \times 10^{-1} \text{ S cm}^{-1}$) of the PEO(90%)/MWNT(10%) although it of the PEO(90%)/DB(10%) is considerably lower ($2.45 \times 10^{-6} \text{ S cm}^{-1}$). Figure 11 showed the electrical conductivity versus increment of total carbon materials content (Δ total carbon materials) in PP(98%)/MWNT(2%) + $n\%$ [PEO(90%)/KB(10%)] or + $n\%$ [PEO(90%)/DBT(10%)] and in PP(98%)/KB(2%) + $n\%$ [PEO(90%)/MWNT(10%)] composites. The PEO(90%)/KB(10%) loading brings about the higher increment rate of the PP(98%)/MWNT(2%) conductivity as compared with the PEO(90%)/DB(10%) one. The difference of the increment rate is due to the higher conductivity of the PEO(90%)/KB(10%). In other words, the electrical quality of the PEO(90%)/KB(10%) connector is higher than that of the PEO(90%)/DB(10%) one. However, the increment rate of the conductivity is considerably slower as compared with those of the PEO/MWNT loadings (see Figure 5). The behavior suggests that it is rather difficult to form the connector between carbon black and MWNT materials. As shown in Figure 11 the PP(98%)/KB(2%) matrix requires much loading amount of the PEO(90%)/MWNT(10%) to increase the conductivity. Form of the KB is spherical, and its aspect ratio is low (ca. 1). Therefore, the formation of connector structure must be hard as compared with the MWNT having the big aspect ratio.

CONCLUSIONS

In this work, the electrical conductivity developments of the PP/MWNT and PB/MWNT were carried out with the PEO/MWNT loading. The conductivity of PP/MWNT was drastically increased by the PEO/MWNT loading. The PB/MWNT conductivity was also able to be improved by the loading although the conductivity improvement effect was lower than that of the PP/MWNT. The Raman spectra showed that the MWNT dispersity state in the PB was lower than that in the PP, resulting that the formation of the PEO/MWNT connector structure required the more loading amount. In addition, the PEO/KB was able to produce the connector structure for the PP/MWNT as well as the PEO/MWNT. These results indicated that the highly conductive composites were producible with the smaller MWNT amounts.

REFERENCES

1. Grimes, C. A.; Dickey, E. C.; Mungle, C.; Ong, K. G.; Qian, D. *J. Appl. Phys.* **2001**, *90*, 4134.
2. Lourie, O.; Cox, D. M.; Wagner, H. D. *Phys. Rev. Lett.* **1998**, *81*, 1638.
3. Yu, M.-F.; Files, B. S.; Arepalli, S.; Ruoff, R. S. *Phys. Rev. Lett.* **2000**, *84*, 5552.
4. Berber, S.; Kwon, Y.-K.; Tománek, D. *Phys. Rev. Lett.* **2000**, *84*, 4613.
5. Valentino, O.; Sarno, M.; Rainone, N. G.; Nobile, M. R.; Ciambelli, P.; Neitzert, H. C.; Simon, G. P. *Phys. E* **2008**, *40*, 2440.
6. Bikiaris, D.; Vassiliou, A.; Chrissafis, K.; Paraskevopoulos, K. M.; Jannakoudakis, A.; Docoslis, A. *Polym. Degrad. Stab.* **2008**, *93*, 952.
7. Ganß, M.; Satapathy, B. K.; Thunga, M.; Weidisch, R.; Pötschke, P.; Jehnichen, D. *Acta Mater.* **2008**, *56*, 2247.
8. Sandler, J. K. W.; Kirk, J. E.; Kinloch, I. A.; Shaffer, M. S. P.; Windle, A. H. *Polymer* **2003**, *44*, 5893.
9. McNally, T.; Pötschke, P.; Halley, P.; Murphy, M.; Martin, D.; Bell, S. E. J.; Brennan, G. P.; Bein, D.; Lemoine, P.; Quinn, J. P. *Polymer* **2005**, *46*, 8222.
10. Gorrasi, G.; Sarno, M.; Bartolomeo, A. D.; Sannino, D.; Ciambelli, P.; Vittoria, V. *J. Polym. Sci. Part B: Polym. Phys.* **2007**, *45*, 597.
11. Valentino, O.; Sarno, M.; Rainone, N. G.; Nobile, M. R.; Ciambelli, P.; Neitzert, H. C.; Simon, G. P. *Phys. E* **2008**, *40*, 2440.
12. Nakatani, H.; Ogura, M.; Yoshikawa, T.; Miyazaki, K.; Okazaki, N.; Terano, M. *Polym. Int.* **2011**, *60*, 1614.
13. Shrivastava, N. K.; Khatua, B. B. *Carbon* **2011**, *49*, 4571.
14. Tang, T.; Huang, B. *J. Polym. Sci. Part B: Polym. Phys.* **1994**, *32*, 1991.
15. Kowalewski, T.; Ragosta, G.; Martuscelli, E.; Galeski, A. *J. Appl. Polym. Sci.* **1997**, *66*, 2047.
16. Nakatani, H.; Miyazaki, K. *J. Appl. Polym. Sci.* **2009**, *112*, 3362.
17. Valentini, L.; Biagiotti, J.; Kenny, J. M.; Santucci, S. *Compos. Sci. Technol.* **2003**, *63*, 1149.